HOKKAIDO UNIVERSITY

Title	Double-Stranded Structure of the Polyinosinic-Polycytidylic Acid Molecule to Elicit TLR3 Signaling and Adjuvant Activity in Murine Intranasal A(H1N1)pdm09 Influenza Vaccination
Author(s)	Nakano, Tetsuo; Ohara, Yuki; Fujita, Hiroshi; Ainai, Akira; Yamamura, Ei-Tora; Suzuki, Tadaki; Hasegawa, Hideki; Sone, Teruo; Asano, Kozo
Citation	DNA and Cell Biology, 39(9), 1730-1740 https://doi.org/10.1089/dna.2019.5324
Issue Date	2020-09-04
Doc URL	http://hdl.handle.net/2115/82612
Rights	Final publication is available from Mary Ann Liebert, Inc., publishers http://dx.doi.org/10.1089/dna.2019.5324
Type	article (author version)
Additional Information	There are other files related to this item in HUSCAP. Check the above URL.
File Information	DNA Cell Biol.39-9_1730-1740.pdf

Instructions for use

Hokkaido University Collection of Scholarly and Academic Papers : HUSCAP

Double-stranded structure of the polyinosinic-polycytidylic acid molecule to elicit TLR3 signaling and adjuvant activity in murine intranasal A(H1N1)pdm09 influenza vaccination

Tetsuo Nakano[1,3*], Yuki Ohara[2], Hiroshi Fujita[1], Akira Ainai[2], Ei-Tora Yamamura[1], Tadaki Suzuki[2], Hideki Hasegawa[2], Teruo Sone[3], and Kozo Asano[3]

[1] *Technical research laboratories, Kyowa Hakko Bio Co., Ltd.*
1-1 Kyowa-cho, Hofu, Yamaguchi 747-8522, Japan.
Phone: +81-835-22-2518

[2] *Department of Pathology, National Institute of Infectious Diseases*
Toyama 1-23-1, Shinjuku-ku, Tokyo 162-8640, Japan.
Phone: +81-3-5285-1111

[3] *Graduate school of agriculture, Hokkaido University*
Kita 9, Nishi 9, Kita-ku, Sapporo, Hokkaido 060-8589, Japan.
Phone: +81-11-706-2493

* Corresponding author: Tetsuo Nakano
Postal Mail Address: Kyowa Hakko Bio Co., Ltd. Research & Business Development Department.
1-9-2 Otemachi, Chiyoda-ku, 100-0004 Tokyo, Japan.
Tel.: +81-3-5205-7303
E-mail: tetsuo.nakano@kyowa-kirin.co.jp

Running title: Impact of poly(I:C) structure on adjuvant activity

Keywords: poly(I:C), double-stranded structure, intranasal vaccination, mucosal adjuvant, immune toxicity, TLR3

Abstract

Polyinosinic-polycytidylic acid (PIC) is a potent dsRNA adjuvant useful in intranasal influenza vaccination. In mice, the intensity and duration of immune responses to PIC correlated with the double-stranded chain length. A rational method to avoid PIC chain extension in PIC production is to use multiple short poly(I) molecules and one long poly(C) molecule for PIC assembly. In this study, we elucidate that a newly developed uPIC100-400 molecule comprising multiple 0.1 kb poly(I) molecules and one 0.4 kb poly(C) molecule effectively enhanced the immune responses in mice, by preventing the challenged viral propagation and inducing hemagglutinin-specific IgA, after intranasal A(H1N1)pdm09 influenza vaccination. Reduced intraperitoneal toxicity of PIC prepared with multiple short poly(I) molecules in mice indicates the widened effective range of uPIC100-400 as an adjuvant. In contrast to uPIC100-400, the PIC molecule comprising multiple 0.05 kb poly(I) molecules failed to elicit mouse mucosal immunity. These results were consistent with TLR3 response but not RIG-I-like receptor response in the cell assays, which suggests that the adjuvant effect of PIC in mouse intranasal immunization depends on TLR3 signaling. In conclusion, the double-stranded PIC with reduced toxicity developed in this study would contribute to the development of PIC-adjuvanted vaccines.

Introduction

Polyinosinic-polycytidylic acid (PIC) molecule is an artificial dsRNA composed of poly(I) and poly(C) that forms a double strand by complementary base-pairing through hydrogen bonds (Chamberlin and Patterson, 1965). This particular homopolymeric dsRNA strongly induces innate immune response in animals (Hilleman *et al.*, 1971), by serving as an adjuvant in prophylactic vaccination against infectious diseases, e.g. influenza (Ichinohe *et al.*, 2010; Ichinohe *et al.*, 2005; Perez-Giron *et al.*, 2014), Ebola virus disease (Phoolcharoen *et al.*, 2011), AIDS (Billeskov *et al.*, 2017), leishmaniasis (Sanchez *et al.*, 2017), bovine respiratory disease (Prysliak and Perez-Casal, 2016), porcine reproductive and respiratory syndrome (Zhang *et al.*, 2013), and Salmonid alphavirus disease (Thim *et al.*, 2012). Especially in intranasal vaccination, PIC is a valuable adjuvant for activation of mucosal immunity in the respiratory tract, improving protection via enhanced dendritic cell function and T cell immunity (Ichinohe *et al.*, 2005; Takaki *et al.*, 2018). The application of PIC as an adjuvant for cancer therapeutic vaccines (Forte *et al.*, 2012; Kano *et al.*, 2016; Seya *et al.*, 2013; Zhao *et al.*, 2019) and a preconditioning agent for brain surgery, with the purpose of inducing tolerance to subsequent ischemia-reperfusion injury, are under study (Gesuete *et al.*, 2012; Li *et al.*, 2015). However, many reports also showed that high-dose or short-term repeated administration of PIC exacerbated some disease symptoms in animal models (Aavani *et al.*, 2015; Graber *et al.*, 2018; Harris *et al.*, 2013; Kanaya *et al.*, 2014; Stowell *et al.*, 2009). Most of these reports did not provide information on the nucleotide length of the double-stranded molecules (NLDS) of PIC used in their studies.

Strengths and durations of immune responses to PIC in mammals are dependent on its NLDS (Field *et al.*, 1970; Machida *et al.*, 1976). In particular, longer NLDS with sedimentation coefficients (S) between 4.2 S and 21.2 S elicit more potent and prolonged immunological responses (Machida *et al.*, 1976). These S values were associated with the NLDS of 0.1–12.7 kbp (Studier, 1965). Furthermore, two PICs with different NLDS elicited distinct innate immune responses in myeloid cells and fibroblasts (Mian *et al.*, 2013). The duration of the action of PIC is usually short because PIC is

easily degraded by ubiquitous RNases in body fluids and blood upon administration to animals (de Clercq, 1979). Therefore, we hypothesized that by using PICs with NLDS within a specific length range and administration of an appropriate dose through an effective route would potentially suppress adverse immune responses caused by some PICs.

However, the NLDS of PIC could not be simply modified by changing the length of poly(I) and poly(C) molecules. Theoretically, annealing of poly(I) and poly(C) molecules of the same length under appropriate conditions would yield a NLDS of the same length to both molecules. However, in practice, multiple poly(I) and poly(C) molecules form one stable double-stranded molecule in a daisy chain. The extended NLDS reaches 5 to 10 times the theoretical NLDS (Hamilton, 1971; Machida *et al.*, 1976). This daisy chained PIC is not easily shortened to its theoretical length even if re-annealing is performed by gentle cooling after heating the sample (Hamilton, 1971; Nakano *et al.*, 2018). Although excessive heating during annealing yields PIC with shortened NLDS, the obtained PIC is an assembly with the mixture of cleaved poly(I) and poly(C) molecules during the excessive heating. This shortened PIC still has limitations regarding the reproducibility of NLDS during production, and storage stability, presumably caused by nicks in the poly(C) strand (Nakano *et al.*, 2018).

In a previous study, we provided a solution to overcome these problems that originated during the PIC production, by constructing a PIC double strand with intact poly(C) and nicked poly(I) strands. Pilot-scale production of PIC with this unevenly nicked double-stranded structure was achieved by annealing multiple short poly (I) molecules into a single poly (C) molecule. The newly developed PIC, uPIC100-400, demonstrated better storage stability than the corresponding evenly structured PIC and the length of this new PIC was also reproducible (Nakano *et al.*, 2018). To our knowledge, this method is the only one that can generate physico-chemically stable NLDS with reproducibility between production lots.

PIC is recognized in mammals by two independent signaling pathways of the innate immunity, resulting in the production of type I interferon (IFN) and proinflammatory cytokines (Takeuchi and Akira, 2009). One is the TLR3–TICAM-1(TRIF) pathway that initiates signaling from TLR3 (Matsumoto *et al.*, 2002; Oshiumi *et al.*, 2003). TLR3 signaling, which starts in the endosomes, is

detected in a wide range of cells, including conventional dendritic cells, macrophages, neural cells, fibroblasts, and epithelial cells (Matsumoto and Seya, 2008). The second one is special a RNA helicase (RLRs)–MAVS pathway that is functionally ubiquitous in various types of cells and initiates signaling in the cytoplasm via dsRNA-captured retinoic acid inducible gene I (RIG-I) and melanoma differentiation associated gene 5 (MDA5) products (Kato *et al.*, 2006; Kawai *et al.*, 2005; Yoneyama *et al.*, 2004). The sensitivity of TLR3 and RLR signaling is regulated independently (Hotz *et al.*, 2015), and innate immune responses derived from these signaling are different (Seya *et al.*, 2013; Seya *et al.*, 2019; Takeuchi and Akira, 2009).

Moreover, poly(I) and poly(C) molecules that constitute poly(I) and poly(C) strands of the PIC double strand influence immune responses against PIC depending on the nucleotide length. A previous study reported that PIC comprising 0.6 kb poly(I) and 0.07 kb poly(C) or larger molecules rendered cells 100% resistant to vesicular stomatitis virus infection upon intravenous injection in New Zealand White rabbits. However, when PIC was composed of 0.6 kb poly(C) and 0.2 kb poly(I) molecules, the cells were 20–50% resistant to the virus (Tytell *et al.*, 1970). Furthermore, the length requirement for inducing a type I IFN response in human L and rabbit kidney cells was more stringent for poly(I) than for the poly(C) molecules (Stewart and De Clercq, 1974). Recent studies using human TLR3-expressing reporter cells and PICs assembled with poly(I) and poly(C) molecules of some lengths indicated that recognition of PICs by human TLR3 was reduced by 75% when shortening either molecule to 30 bases (Okahira *et al.*, 2005). Thus, the effects of both poly(I) and poly(C) lengths of PIC on the innate immune response remain controversial.

In this study, we investigated the effect of poly(I) and poly(C) length on the immune response in mice by administering PICs assembled with poly(I) and poly(C) molecules of varying molecule lengths as adjuvants during intranasal influenza vaccination. We demonstrated the effect of poly(I) length of PIC on the innate immune response. Specifically, a successful activity and also expanded effective range of PIC as adjuvant were obtained after intranasal influenza vaccination of mice with PIC structures of uneven lengths.

Materials and Methods

PICs and reagents

PICs used in this study are listed in Table 1. Preparation and purification methods of these PICs were previously described in detail (Nakano *et al.*, 2018). Briefly, poly(I) and poly(C) molecules of various lengths were enzymatically synthesized without a template by polynucleotide phosphorylase (PNPase) from IDP and CDP, respectively. The desired nucleotide lengths of both poly(I) and poly(C) molecules were obtained by adjusting the endpoint of the PNPase reaction and monitoring their lengths. PIC was prepared by annealing poly(I) to poly(C), either by mixing them at 20–25°C (Field *et al.*, 1967) or by mixing and cooling the mix to 20–25°C after heating to 60–70°C (Hamilton, 1971; Torrence, 1981). The mixture ratio of poly(I) to poly(C) was 52:48, according to the absorbance at 260 nm (OD_{260}), as determined on the basis of a reduction in the OD_{260} due to decreasing the sum of base and base pair after mixing poly(I) and poly(C) (Chamberlin and Patterson, 1965). The average nucleotide length of poly(I), poly(C), and PIC molecules was determined by size exclusion chromatography (SEC), as previously described (Nakano *et al.*, 2018). The long-chain PIC was purchased from GE Healthcare Life Sciences (Buckinghamshire, England). Chloroquine was obtained from Wako Pure Chemical Corp. (Tokyo, Japan). Human serum was provided by Lonza Japan Ltd. (Tokyo, Japan)

Mice, vaccine, and virus

Female BALB/c mice of 6 to 8-week postnatal age, purchased from Japan SLC (Hamamatsu, Shizuoka, Japan), were used for vaccination studies. Mice were kept under specific-pathogen-free conditions in the animal facility at National Institute of Infectious Diseases (Tokyo, Japan). Mouse-adapted influenza virus A/Narita/1/09 (H1N1)pdm09 used in this study was propagated in the allantoic cavities of 10- to 11-day-old fertile chicken eggs for 2 days at 37 °C (Ainai *et al.*, 2015). Split-virus vaccine prepared from A/California/7/09 (X-179A) (H1N1)pdm09, a reassortant vaccine strain derived

from A/California/7/09 (H1N1)pdm09 virus, was kindly provided by the Research Foundation for Microbial Disease of Osaka University (BIKEN, Kanonji, Kagawa, Japan).

The melting temperature analysis

The melting temperature (*Tm*) was determined from the temperature dissociation curve of OD_{260}, which was measured using a TMSPC-1 system (SHIMADZU, Kyoto, Japan). Sample preparation was performed by dissolving RNAs in PBS (pH 7.4) and adjusting the concentration to 0.5 OD_{260} units.

Cell culture experiments

Evaluation of the human TLR3, mouse TLR3, and mouse RLRs responses were performed by using the HEK-Blue™ hTLR3, the HEK-Blue™ mTLR3, and the C57/WT MEF Cell Systems (InvivoGen, CA, USA), respectively, at the recommended conditions. The human lung fibroblast MRC-5 cell line (RCB0218) (Billiau *et al.*, 1977), obtained from the RIKEN BRC through the National Bio-Resource Project of the MEXT, was used for testing the innate immune response. Cell cultures were maintained at 37°C in 5% CO_2, using DMEM supplemented with 10% fetal bovine serum (FBS), and the corresponding antibiotics for the different cell systems. Collagen-coated plates were used for culturing the HEK-Blue™ hTLR3 and the HEK-Blue™ mTLR3 cell systems. In our experiments, the cells were grown to pre-confluency on 12-well plates, washed three times with serum-free DMEM, and finally incubated with 1 mL of the same washing solution just before PIC addition. A total of 0.1 μg of PIC naked form was added to each well containing the HEK-Blue™ hTLR3 or the HEK-Blue™ mTLR3 cells. In the experiments containing C57/WT MEFs and MRC-5 cells, 50 μL of the liposomal PIC mixture prepared with 1 μg of PIC and a cationic liposome LyoVec™ (InvivoGen) were added to each well unless otherwise noted. For untransfected control cells, 50 μL of a liposomal mixture prepared with saline and LyoVec™ was added to each well. After incubation for 2 h, 0.1 mL of low-IgG FBS (Life Technologies Japan, Tokyo, Japan) was added to each well, and the culture continued for 20 h unless otherwise noted. In the experiments with the HEK-Blue™ hTLR3, HEK-Blue™

mTLR3, and C57/WT MEF cells, the levels of secreted alkaline phosphatase (SEAP) induced by the corresponding signaling pathways were determined using QUANTI-Blue™ (InvivoGen). The IFN-β concentration in the MRC-5 culture was determined using the human-IFN-β ELISA Kit (Kamakura Techno-Science, Kanagawa, Japan). Cell viability was measured by using the Premix WST-1 Cell Proliferation Assay System (Takara-Bio, Shiga, Japan).

A focused-DNA microarray analysis

MRC-5 cells were cultured in 60-mm dishes for DNA microarray analysis. Culture conditions were the same as those for 12-well plates; however, the volumes of culture media and liposomal mixture were increased 5-fold. Total RNA was isolated from MRC-5 cells cultured 24 h after transfection with PIC, using RNeasy Mini Kit (Qiagen, Hilden, Germany). A focused DNA microarray analysis using Genopal™ Human Innate Immunity Chip (Mitsubishi Chemical, Tokyo, Japan) was performed by a contract research organization (Kurabo Industries, Osaka, Japan).

Intranasal influenza vaccination and influenza virus challenge study in mice

Mice were vaccinated twice at a 3-week interval with 10–100 ng hemagglutinin (HA) of split-virus vaccine with or without PICs. Intranasal vaccination was performed by administration of 5 μL vaccine solution into each nostril (total 10 μL per mouse). Subcutaneous vaccination was performed by injecting 100 μL of split-virus vaccine solution into the dorsal part of the cervical region. All mice were challenged with mouse-adapted A/Narita/1/09 (H1N1)pdm09 virus, 2 weeks after the last vaccination. Infection was performed by administering 2 μL of a suspension containing the virus in each nostril (total 4 μL, 40,000 plaque-forming units [PFUs] per mouse). At 3 days post-infection, all mice were sacrificed, and serum and nasal wash samples were collected for determination of antibody levels and virus titers. Nasal wash samples were obtained from mice by washing the nasal cavities of the isolated upper heads with 1 mL of PBS containing 0.1% bovine serum albumin and antibiotics. Vaccinations and viral infections were performed under anesthesia.

The virus titers of nasal washes were measured according to the method previously described (Tobita, 1975). Briefly, 200 μL aliquots of serial 10-fold dilutions of the nasal wash fluid were inoculated into MDCK cells in six-well plates. After 1 h of incubation, 2 mL of agar medium was overlaid into each well. The number of plaques in each well was counted after 2 days in cell culture. HA-specific nasal IgA and serum IgG antibody levels were determined by ELISA as previously described (Asahi *et al.*, 2002). Standards for HA-specific IgA and IgG antibody titrations were prepared from the nasal washes and sera collected from mice intranasally hyper-immunized with HA vaccine in the presence of long-chain PIC (GE Healthcare Life Sciences) and expressed in the same arbitrary units (160-unit).

Animal studies were performed in strict accordance with the Guidelines for Proper Conduct of Animal Experiments of the Scientific Council of Japan. All animal experiments were conducted in strict compliance with animal husbandry and welfare regulations in biosafety level two animal facilities, according to the guidelines of the Animal Care and Use Committee of the National Institute of Infectious Diseases.

Single-dose toxicity studies in mice

Single-dose toxicity studies were performed by Research Institute for Animal Science Biochemistry and Toxicology (RIAS, Kanagawa, Japan), a contract research organization. Male Crlj:CDl (ICR) mice at postnatal age of 6 weeks, purchased from Charles River Laboratories Japan (Yokohama, Japan), were used. These mice were kept in a temperature and humidity-controlled environment under a 12 h light–dark cycle with free access to food and water in the barrier facilities at RIAS. Mice were intraperitoneally injected with 20 mL/kg of PICs dissolved in sterile saline solution with gamma sterilized 25G x 1 needle (n = 5/group). Each mouse received PIC solution according to its body weight. Mice were observed for appearance and behavior twice a day, and body weight and food consumption were measured once a day for 7 days. Surviving animals were euthanized by carbon dioxide gas and necropsied on the last day.

These animal studies were performed in strict accordance with the Guidelines for Proper Conduct of Animal Experiments of the Scientific Council of Japan. All experimental design and procedures were approved as by the Animal Care and Use Committee of RIAS and performed in strict compliance with the Animal Experiments Regulations of RIAS (authorization No. 12-086 and 12-137).

PIC digestion with serum

A total of 10 µl of human serum (Lonza Japan, Tokyo, Japan) diluted to one tenth was added to 90 µl of 0.1 mg/ml PICs solution dissolved in PBS (pH 7.4), then incubated for 5 min at 37 °C. RNase activity in each reaction mixture was inactivated by Phenol/Chloroform extraction. The length distribution of PICs in the aqueous layer was analyzed by agarose gel electrophoresis.

Statistical analysis

Statistical analysis for cell culture and single-dose toxicity studies were performed using SPSS Statics statistical software (SPSS Inc., IL, USA). One-way analysis of variance (ANOVA) was applied to compare means among groups. Post-hoc pairwise comparisons were conducted using Tukey's test. The LD_{50} of PICs in mice were estimated by logistic regression. Statistical analysis for vaccination studies was performed using GraphPad Prism statistical software (GraphPad Software Inc., CA, USA). Viral titers were compared using Kruskal-Wallis tests with Dunn’s multiple comparison tests, and antibody response results were compared using one-way ANOVA with Bonferroni’s multiple comparison tests. Data were considered statistically significant if the p-values were less than 0.05.

Results

Effect of nucleotide length of poly(I) and poly(C) molecules on TLR3 recognition

The uneven-structured PIC in this paper refers to a PIC molecule that is composed by one poly(C) molecule with the same nucleotide length to the target NLDS and multiple poly(I) molecules with shorter nucleotide lengths than that of the poly(C) molecule, unless otherwise specified. A representative uneven-structured of PIC is uPIC100-400, which is assembled by annealing four poly(I) molecules of 0.1 kb to one poly(C) molecule of 0.4 kb. The structural differences between uPIC100-400 and PIC400-400CA, a conventional structured PIC which has the same dsRNA average length, are illustrated (Fig. 1). In order to investigate whether the length of the poly(I) molecule influenced the PIC immunological activity, the TLR3 signaling response was evaluated using human TLR3 reporter cells. TLR3 signaling was prominent in cells treated with PIC molecules comprising poly(I) molecules of 0.07 kb–0.4 kb and a poly(C) molecule of 0.4 kb, or PIC molecules comprising poly(I) molecules of 0.4 kb and a poly(C) molecule of 0.05 kb–0.1 kb ($p < 0.001$). Intensity of the TLR3 signaling of these PICs was not significantly different from that of PIC400-400CA, except for uPIC70-400, which was composed by poly(I) molecules of 0.07 kb. On the other hand, no significant TLR3 signaling response was generated by addition of uPIC50-400 composed of 0.05 kb poly(I) molecules (Fig. 2A). The same results were also observed in the mouse TLR3 reporter cell assay (Fig. 2B). These results indicated that the decrease of TLR3 signaling was characteristic of PIC molecules comprised of poly(I) molecule with 0.07 kb or less.

Effect of nucleotide length of poly(I) and poly(C) molecules on RLRs recognition

RLR response to PIC was evaluated using C57/WT MEF reporter cells. The SEAP production, resulting from the sum of RIG-I and MDA5 signals, was significantly increased after transfection of the cells with PIC using cationic liposomes. There was no significant difference in SEAP induction rate of PIC-transfected cells with poly(I) molecule of 0.05 kb–0.4 kb (Fig. 3).

The response of RNA helicases was also evaluated using the human lung fibroblast cell line MRC-5. IFN-β production was only observed in response to transfection of the MRC-5 cells with PIC by using cationic liposomes. Naked PIC did not induce IFN-β production of MRC-5 cells even when the amount of PIC increased by 100-fold in our experimental conditions (Fig. 4). No significant difference in the effects of PICs assembled with poly(I) and poly(C) molecules of different lengths on IFN-β production was observed in the PIC-transfected MRC-5 culture.

Effect of PIC poly(I) and poly(C) nucleotide length on the expression of genes related to innate immunity

Considering that PIC molecules undergo RNase enzymatic cleavage at the phosphodiester bond of both poly(I) and poly(C) strands leading to small oligoribonucleotides during and after intracellular entry, a mix of ssRNA and dsRNA fragments was generated. This heterogenous mix of oligoribonucleotides might have caused differences in the innate immunity response. To rule out this speculation, we investigated the expression of the genes involved in innate immunity after MRC-5 cells were transfected with PIC by using a focused DNA microarray. Alterations in the gene expression of MRC-5 cells at 24 h post-transfection with PIC are shown in scatter plots (Fig. 5). In PIC400-400CA-transfected cells, expression of 166 out of 199 studied genes were up-regulated with a significant difference of > 3 standard deviation in a comparative analysis against untransfected cells. Expression of none of the analyzed genes was significantly down-regulated (Fig. 5A). Among the up-regulated genes, gene expression of RIG-I (DDX58, 72 fold), MDA5 (IFIH1, 98 fold), IFN-β (IFNB1, 173 fold), IFN-inducible proteins (10–1000 fold), and some inflammatory chemokines such as CCL5 (534 fold) and cytokines as IL-6 (238 fold) were significantly affected. Remarkably, TLR3 gene expression was up-regulated by 173-fold. Gene up-regulation, in fold changes, after transfection of cells with PIC400-400CA was highly correlated to that with uPIC100-400 (R^2 = 0.964), uPIC50-400 (R^2 = 0.978), or ruPIC400-50 (R^2 = 0.967) (Fig. 5B–D). The similarity of gene responses between all the experimental conditions at 24 h after transfection of cells with PIC raised a question about the

possibility of convergent gene responses at late stages of cell death resulting from necrosis. To rule out this possibility, DNA microarray was also investigated in cells cultured for 4 h after PIC transfection, when the IFN-β production first appeared (Supplementary Fig. S1). The gene expression was compared among the cells transfected with two lots of PIC400-400CA and two lots of uPIC50-400 and untransfected cells. Correlation of gene expressions between untransfected and PIC-transfected cells after 4 h in culture was $R^2 = 0.867 \pm 0.014$ (n = 4), which was higher than after 24 h culture with $R^2 = 0.454 \pm 0.006$ (n = 4); however, it was lower than that of gene expression after 4 h of PIC production from both sources ($R^2 = 0.968 \pm 0.010$; n = 2), and that between PIC400-400CA and uPIC50-400 ($R^2 = 0.975 \pm 0.012$; n = 4). These results indicated that the gene responses were generated in PIC-transfected fresh cells, but no significant difference on gene expression between PIC400-400CA-transfected and uPIC50-400-transfected fresh cells. Therefore, the similarity in genetic responses between the cells cultured for 24 h after transfected by PICs did not result from convergent gene responses at a late stages of cell death. As a conclusion, the PIC biological effect on human fibroblast cells after transfection was not affected by the length of PIC poly(I) and poly(C) molecules at least between 0.05 kb and 0.4 kb.

Evaluation of PICs as vaccine adjuvant for an intranasal A(H1N1)pdm09 influenza vaccine in mice

In order to investigate the *in vivo* efficacy of the uneven-structured PIC as an intranasal vaccine adjuvant, uPIC100-400 and uPIC50-400 were evaluated using the mouse model of intranasal influenza vaccination. The titer of challenged A(H1N1)pdm09 influenza virus collected from nasal washes of mice which received two intranasal doses of long-chain PIC-adjuvanted vaccine was significantly suppressed to 1/1000, compared to that of mice which received two intranasal doses of PIC-free vaccine (Fig. 6A). No significant suppression of the virus titer was observed in the groups subcutaneously vaccinated with the same amount of A(H1N1)pdm09 influenza antigen with or without PICs (Fig. 6B). These results confirmed those obtained in previous reports which examined long-chain PIC as adjuvants of intranasal influenza vaccination (Ichinohe *et al.*, 2010; Ichinohe *et al.*, 2005). In a

concurrent evaluation, significant suppression of the challenged A(H1N1)pdm09 influenza virus expansion was also observed after both intranasal vaccination supplemented with 10 μg of PIC400-400CA and 10 μg of uPIC100-400 (Fig. 6A). Both molecules, PIC400-400CA and uPIC100-400, suppressed further the challenged virus expansion in a dose-dependent manner at the same level, which indicated that the adjuvant activity of PIC was not affected by the shortening of the poly(I) molecules to 0.1 kb. The lower adjuvant activity of both PIC400-400CA and uPIC100-400, compared to that of the long-chain PIC, was probably caused by shorter NLDS. On the other hand, the uPIC50-400-adjuvanted vaccine did not suppress the challenged virus expansion, indicating a critical difference in the *in vivo* adjuvant activity between uPIC100-400 and uPIC50-400.

The responses of the HA-specific IgA levels in nasal washes and the HA-specific IgG levels in serum were ambiguous, as shown in Fig. 6A. However, both antibody responses were clearly detected in the additional experiment in which the dose of the HA antigen was increased to 100 ng. Both the IgA and IgG responses were significantly increased in the mouse group receiving the intranasal vaccination supplemented with 10 μg of the long-chain PIC and 20 μg of uPIC100-400, and were correlated to the reductions of virus titer in the nasal wash (Fig. 6C).

Single-dose toxicity of PICs in mice

Single-dose toxicities in mice were examined for the four structures of PIC molecule with different lengths of poly(I) molecules (Table 2). It is known that PIC is relatively nontoxic to animals by intranasal administration, and the intraperitoneal toxicity data were used instead to discuss the effective dose of intranasal PIC administration compared to acute toxicity (Field, 1973). Therefore, we conducted mouse intraperitoneal administration studies to evaluate signs of immunological toxicity.

Mice receiving 100 mg/kg of long-chain PIC administration (a control group) experienced severe weight loss, piloerection, perianal dirt, necrosis of the tail tip, decreased locomotor activity, and blepharoptosis. Acute toxicity was not observed, but three out of five mice died between days 1 and 4. In the concurrent study, mice administered with 100 mg/kg of PIC400-400CA evidenced the same

symptoms to the group receiving the long-chain PIC administration, except for decreased locomotor activity. One out of five mice died at day 4. On the other hand, mice administrated with 100 mg/kg of uPIC200-400CA, uPIC100-400, or uPIC50-400 only showed transient weight loss, and either piloerection or perianal dirt. No deaths were observed in these groups. Transient weight loss after PIC administration decreased in the following order: uPIC50-400, uPIC100-400, uPIC200-400CA, and PIC400-400CA (Supplementary Fig. S2), suggesting a decrease in immunological toxicity due to the shortened poly(I) molecules. Also, an intraperitoneal administration study was conducted with increasing concentrations of the four PICs (Table 2). In the case of PIC400-400CA, all 5 mice died in the group receiving 200 mg/kg. On the other hand, the same mortality rate was observed in mice injected with double amount of uPIC200-400CA and uPIC100-400, 400 mg/kg administration, compared to 200 mg/kg. The intraperitoneal toxicity of uPIC50-400 was minimal among the PICs tested, and the mortality rate at doses of 200 mg/kg and 400 mg/kg were 0/5 and 2/5, respectively. The intraperitoneal LD_{50} of PIC400-400CA, uPIC200-400CA, uPIC100-400, and uPIC50-400 were estimated at 120 mg/kg ($p < 0.05$), 190 mg/kg ($p < 0.001$), 210 mg/kg ($p < 0.001$), and 280 mg/kg ($p < 0.234$), respectively, by logistic regression. The LD_{50} of the long-chain PIC was not determined by logistic regression, but it was estimated to be less than 100 mg/kg.

Discussion

We have demonstrated that the uneven structure of uPIC100-400 was appropriate as an adjuvant of intranasal A(H1N1)pdm09-inactivated influenza vaccine to use in mice challenge studies. Administration of uPIC100-400 exhibited a significant enhancement of immune response equivalent to that elicited by the conventional PIC400-400CA structure. On the other hand, the other tested uneven-structured uPIC50-400 molecules failed to enhance the immune response of mice in the concurrent studies. These results indicated that the structural requirement on the length of poly(I) molecules was 0.1 kb or more to enhance the efficacy of intranasal influenza vaccination. An equivalent adjuvant activity between uPIC100-400 and PIC400-400CA, as a difference to that of uPIC50-400 which was inferior, was observed in mice receiving intranasal vaccination according to the TLR3 reporter cell experiments, but in disagreement with the results derived from the RLRs reporter cell experiments. These results suggested no or slight involvement of RLRs in the adjuvant effect of naked PIC in mouse intranasal influenza vaccination.

Double increase in mice intraperitoneal LD_0 and LD_{50} by going from PIC400-400CA to uPIC100-400 and an equivalent adjuvant activity in intranasal influenza vaccination suggested double expansion on the effective range of uPIC100-400 to PIC400-400CA. The structural difference between uPIC100-400 and PIC400-400CA was the length of composed poly(I) molecule in the double strand. Biodegradation of PIC in serum showed uPIC100-400 strands primarily forming shorter fragments than PIC400-400CA molecules, followed by random digestion; meanwhile, the fragments derived from uPIC50-400 were much shorter than those of uPIC100-400 (Supplementary Fig. S3). Based on the fact that the major RNase activity in serum was about 100 times more active against poly(C) than poly(I) molecules (de Clercq, 1979), the nicks in poly(I) strand may be preferentially breakage points of PIC *in vivo*. The prompt fragmentations of uPIC100-400 and uPIC50-400 by RNases presumably resulted in reduced toxicity due to shorter period of innate immune stimulation.

A focused DNA microarray analysis of human fibroblast MRC-5 cells revealed that the difference of structure in uPIC100-400, uPIC50-400, and ruPIC400-50 did not influence the expression of the genes involved in innate immunity after transfection. In other words, an equal gene response after delivering PIC molecules with different nicks in both strands with varying poly(I) and poly(C) molecule lengths in cells indicated that nicks in the strands did not influence the quality of innate immune response. Importantly, TLR3 gene was involved in the significant up-regulation of genes after cells were transfected with PIC using LyoVec™ (Invivogen), which suggested that the TLR3 signaling was generated during such delivery. The equivalency in TLR3 gene up-regulation by uPIC50-400 and by the other PICs suggested that uPIC50-400 could initiate TLR3 signaling if delivered into cells. This conjecture was supported by the results that IFN-β production by the uPIC50-400-transfected cells was partially inhibited by chloroquine, an endosomal TLR3 inhibitor (Supplementary Fig. S4). The dose-dependent inhibition rate by chloroquine was similar to that of transfection with uPIC100-400, and was in accordance with the dose-dependent inhibition of long-chain PIC-induced IFN-β mRNA expression obtained in human corneal epithelial cells (Kumar *et al.*, 2006). It was found that uPIC50-400 exerted strong adjuvant activity in intranasal A(H1N1)pdm09-inactivated influenza vaccination in mice when it was conjugated to cationic rod shape gold nanoparticles (Tazaki *et al.*, 2018), possibly by delivering the PIC molecules to certain cells located in the nasal cavity, that evoked successful TLR3 signaling.

Adjuvant activities of both uPIC100-400 and PIC400-400CA in intranasal A (H1N1)pdm09-inactivated influenza vaccination in mice were inferior to those of long-chain PIC molecules. However, dose-dependent efficacy was observed in both uPIC100-400 and PIC400-400CA, and it was demonstrated that using double the amount of uPIC100-400 could overcome the low efficacy against the long-chain PIC. Double or higher amount of uPIC100-400 is probably acceptable in terms of toxicity, based on toxicity results of intraperitoneal experiments in mice. Also, increase of uPIC100-400 concentration to 25 mg/ml or more can be still mixed with the vaccine without significantly affecting the viscosity of PIC solution. However, high viscosity of long-chain PIC at concentrations above 5 mg/mL prevents to its use.

The decreased TLR3 signaling observed with uPIC50-400 was probably not due to a reduced binding force between strands of the uPIC50-400 double strand, because ruPIC400-50, which has the opposite length for both poly(I) and poly(C) molecules, had a lower *Tm* value than uPIC50-400 but induced equivalent TLR3 signaling to PIC400-400CA. These results indicate no relationship between the *Tm* values and the induction of TLR3 signaling. Nicks in the poly(I) strand of uPIC50-400 at short intervals resulted in shortened fragmentation of the double strand by RNase treatment (Supplementary Fig. S3), which may be the reason for the lack of TLR3 signaling induction.

Conclusion

In summary, using uneven molecular structures of the PIC strands is the key to reduce immunological toxicity of PICs after administration. The uPIC100-400 exhibited an adjuvant activity equivalent to the conventional PIC400-400CA in mouse intranasal influenza vaccination, and approximately half intraperitoneal toxicity, which indicated a double effective range of uPIC100-400. To confirm the efficacy of uPIC100-400 during intranasal vaccination and to eliminate potential adverse events, further *in vivo* studies are required.

Acknowledgments

The authors would like to thank Yumiko Morita, Nozomi Hayashida, Takahiro Iguchi, and Koushirou Tabata for technical assistance, as well as Yuzuru Yamamoto, Atsushi Noda, and Masaya Ito (Research Institutes for Animal Science in Biochemistry and Toxicology) for helpful advice on mouse toxicity studies.

The work was supported in part by a Grant-in-Aid for Research on Emerging and Reemerging Infectious Diseases from the Japanese Ministry of Health, Labor, and Welfare and the Japan Agency for Medical Research and Development (AMED) under grant numbers JP19fk0108051 and JP19fk0108083. The funding agencies had no role in the study design, data collection and analysis, decision to publish, or preparation of the manuscript.

Disclosure

No competing financial interests to disclose.

References

Aavani T., Rana S.A., Hawkes R., Pittman Q.J. (2015). Maternal immune activation produces cerebellar hyperplasia and alterations in motor and social behaviors in male and female mice. Cerebellum **14,** 491-505.

Ainai A., Hasegawa H., Obuchi M., Odagiri T., Ujike M., Shirakura M., *et al.* (2015). Host Adaptation and the Alteration of Viral Properties of the First Influenza A/H1N1pdm09 Virus Isolated in Japan. PLoS One **10,** e0130208.

Asahi Y., Yoshikawa T., Watanabe I., Iwasaki T., Hasegawa H., Sato Y., *et al.* (2002). Protection against influenza virus infection in polymeric Ig receptor knockout mice immunized intranasally with adjuvant-combined vaccines. J Immunol **168,** 2930-2938.

Billeskov R., Wang Y., Solaymani-Mohammadi S., Frey B., Kulkarni S., Andersen P., *et al.* (2017). Low Antigen Dose in Adjuvant-Based Vaccination Selectively Induces CD4 T Cells with Enhanced Functional Avidity and Protective Efficacy. J Immunol **198,** 3494-3506.

Billiau A., Edy V.G., Heremans H., Van Damme J., Desmyter J., Georgiades J.A., *et al.* (1977). Human interferon: mass production in a newly established cell line, MG-63. Antimicrob Agents Chemother **12,** 11-15.

Chamberlin M.J., Patterson D.L. (1965). Physical and chemical characterization of the ordered complexes formed between polyinosinic acid, polycytidylic acid and their deoxyribo-analogues. J Mol Biol **12,** 410-428.

de Clercq E. (1979). Degradation of poly(inosinic acid) - poly(cytidylic acid) [$(I)_n$ - $(C)_n$] by human plasma. Eur J Biochem **93,** 165-172.

Field A.K., Tytell A.A., Lampson G.P., Hilleman M.R. (1967). Inducers of interferon and host resistance, II. Multistranded synthetic polynucleotide complexes. Proc Natl Acad Sci U S A **58,** 1004-1010.

Field A.K., Tytell A.A., Lampson G.P., Nemes M.M., Hilleman M.R. (1970). Double-stranded polynucleotides as interferon inducers. J Gen Physiol **56,** 90-96.

Field A.K. (1973). Interferon induction by polynucleotides. In *Selective inhibitors of viral functions* Carter W.A. ed. (CRC press, Cleveland) pp. 149-176.

Forte G., Rega A., Morello S., Luciano A., Arra C., Pinto A., *et al.* (2012). Polyinosinic-polycytidylic acid limits tumor outgrowth in a mouse model of metastatic lung cancer. J Immunol **188,** 5357-5364.

Gesuete R., Packard A.E., Vartanian K.B., Conrad V.K., Stevens S.L., Bahjat F.R., *et al.* (2012). Poly-ICLC preconditioning protects the blood-brain barrier against ischemic injury in vitro through type I interferon signaling. J Neurochem **123 Suppl 2,** 75-85.

Graber T.G., Rawls B.L., Tian B., Durham W.J., Brightwell C.R., Brasier A.R., *et al.* (2018). Repetitive TLR3 activation in the lung induces skeletal muscle adaptations and cachexia. Exp Gerontol **106,** 88-100.

Hamilton L.D. (1971). Immunogenic polynucleotides. In *Biological effects of polynucleotides.* Roland F. Beers J., Braun W. eds. (Springer-Verlag, New York) pp. 107-128.

Harris P., Sridhar S., Peng R., Phillips J.E., Cohn R.G., Burns L., *et al.* (2013). Double-stranded RNA induces molecular and inflammatory signatures that are directly relevant to COPD. Mucosal immunology **6,** 474-484.

Hilleman M.R., Lampson G.P., Tytell A.A., Field A.K., Nemes M.M., Krakoff I.H., *et al.* (1971). Double-stranded RNAs in relation to interferon induction and adjuvant activity. In *Biological Effects of Polynucleotides.* Roland F. Beers J., Braun W. eds. (Springer-Verlag, New York) pp. 27-44.

Hotz C., Roetzer L.C., Huber T., Sailer A., Oberson A., Treinies M., *et al.* (2015). TLR and RLR Signaling Are Reprogrammed in Opposite Directions after Detection of Viral Infection. J Immunol **195,** 4387-4395.

Ichinohe T., Ainai A., Ami Y., Nagata N., Iwata N., Kawaguchi A., *et al.* (2010). Intranasal administration of adjuvant-combined vaccine protects monkeys from challenge with the highly pathogenic influenza A H5N1 virus. J Med Virol **82,** 1754-1761.

Ichinohe T., Watanabe I., Ito S., Fujii H., Moriyama M., Tamura S., *et al.* (2005). Synthetic double-stranded RNA poly(I:C) combined with mucosal vaccine protects against influenza virus infection. J Virol **79,** 2910-2919.

Kanaya K., Kondo K., Suzukawa K., Sakamoto T., Kikuta S., Okada K., *et al.* (2014). Innate immune responses and neuroepithelial degeneration and regeneration in the mouse olfactory mucosa induced by intranasal administration of Poly(I:C). Cell Tissue Res **357,** 279-299.

Kano Y., Iguchi T., Matsui H., Adachi K., Sakoda Y., Miyakawa T., *et al.* (2016). Combined adjuvants of poly(I:C) plus LAG-3-Ig improve antitumor effects of tumor-specific T cells, preventing their exhaustion. Cancer Sci **107,** 398-406.

Kato H., Takeuchi O., Sato S., Yoneyama M., Yamamoto M., Matsui K., *et al.* (2006). Differential roles of MDA5 and RIG-I helicases in the recognition of RNA viruses. Nature **441,** 101-105.

Kawai T., Takahashi K., Sato S., Coban C., Kumar H., Kato H., *et al.* (2005). IPS-1, an adaptor triggering RIG-I- and Mda5-mediated type I interferon induction. Nat Immunol **6,** 981-988.

Kumar A., Zhang J., Yu F.-S.X. (2006). Toll-like receptor 3 agonist poly(I:C)-induced antiviral response in human corneal epithelial cells. Immunology **117,** 11-21.

Li Y., Xu X.L., Zhao D., Pan L.N., Huang C.W., Guo L.J., *et al.* (2015). TLR3 ligand Poly IC Attenuates Reactive Astrogliosis and Improves Recovery of Rats after Focal Cerebral Ischemia. CNS Neurosci Ther **21,** 905-913.

Machida H., Kuninaka A., Yoshino H. (1976). Relationship between the molecular size of poly I-poly C and its biological activity. Jpn J Microbiol **20,** 71-76.

Matsumoto M., Kikkawa S., Kohase M., Miyake K., Seya T. (2002). Establishment of a monoclonal antibody against human Toll-like receptor 3 that blocks double-stranded RNA-mediated signaling. Biochem Biophys Res Commun **293,** 1364-1369.

Matsumoto M., Seya T. (2008). TLR3: interferon induction by double-stranded RNA including poly(I:C). Adv Drug Deliv Rev **60,** 805-812.

Mian M.F., Ahmed A.N., Rad M., Babaian A., Bowdish D., Ashkar A.A. (2013). Length of dsRNA (poly I:C) drives distinct innate immune responses, depending on the cell type. J Leukoc Biol **94,** 1025-1036.

Nakano T., Yamamura E.-T., Fujita H., Sone T., Asano K. (2018). Novel methods for nucleotide length control in double-stranded polyinosinic-polycytidylic acid production using uneven length components. Bioscience, Biotechnology, and Biochemistry **82,** 1889-1901.

Okahira S., Nishikawa F., Nishikawa S., Akazawa T., Seya T., Matsumoto M. (2005). Interferon-beta induction through toll-like receptor 3 depends on double-stranded RNA structure. DNA Cell Biol **24,** 614-623.

Oshiumi H., Matsumoto M., Funami K., Akazawa T., Seya T. (2003). TICAM-1, an adaptor molecule that participates in Toll-like receptor 3-mediated interferon-beta induction. Nat Immunol **4,** 161-167.

Perez-Giron J.V., Belicha-Villanueva A., Hassan E., Gomez-Medina S., Cruz J.L., Ludtke A., *et al.* (2014). Mucosal polyinosinic-polycytidylic acid improves protection elicited by replicating influenza vaccines via enhanced dendritic cell function and T cell immunity. J Immunol **193,** 1324-1332.

Phoolcharoen W., Dye J.M., Kilbourne J., Piensook K., Pratt W.D., Arntzen C.J., *et al.* (2011). A nonreplicating subunit vaccine protects mice against lethal Ebola virus challenge. Proc Natl Acad Sci U S A **108,** 20695-20700.

Prysliak T., Perez-Casal J. (2016). Immune responses to Mycoplasma bovis proteins formulated with different adjuvants. Can J Microbiol **62,** 492-504.

Sanchez M.V., Elicabe R.J., Di Genaro M.S., Germano M.J., Gea S., Garcia Bustos M.F., *et al.* (2017). Total Leishmania antigens with Poly(I:C) induce Th1 protective response. Parasite Immunol **39,** e12491.

Seya T., Azuma M., Matsumoto M. (2013). Targeting TLR3 with no RIG-I/MDA5 activation is effective in immunotherapy for cancer. Exp Op Ther Tar **17,** 533-544.

Seya T., Takeda Y., Matsumoto M. (2019). A Toll-like receptor 3 (TLR3) agonist ARNAX for therapeutic immunotherapy. Adv Drug Deliv Rev **147,** 37-43.

Stewart W.E., 2nd, De Clercq E. (1974). Relationship of cytotoxicity and interferon-inducing activity of polyriboinosinic acid. Polyribocytidylic acid to the molecular weights of the homopolymers. J Gen Virol **23,** 83-89.

Stowell N.C., Seideman J., Raymond H.A., Smalley K.A., Lamb R.J., Egenolf D.D., *et al.* (2009). Long-term activation of TLR3 by poly(I:C) induces inflammation and impairs lung function in mice. Respir Res **10,** 43.

Studier F.W. (1965). Sedimentation studies of the size and shape of DNA. J Mol Biol **11,** 373-390.

Takaki H., Kure S., Oshiumi H., Sakoda Y., Suzuki T., Ainai A., *et al.* (2018). Toll-like receptor 3 in nasal CD103(+) dendritic cells is involved in immunoglobulin A production. Mucosal Immunol **11,** 82-96.

Takeuchi O., Akira S. (2009). Innate immunity to virus infection. Immunol Rev **227,** 75-86.

Tazaki T., Tabata K., Ainai A., Ohara Y., Kobayashi S., Ninomiya T., *et al.* (2018). Shape-dependent adjuvanticity of nanoparticle-conjugated RNA adjuvants for intranasal inactivated influenza vaccines. RSC Advances **8,** 16527-16536.

Thim H.L., Iliev D.B., Christie K.E., Villoing S., McLoughlin M.F., Strandskog G., *et al.* (2012). Immunoprotective activity of a Salmonid Alphavirus Vaccine: comparison of the immune responses induced by inactivated whole virus antigen formulations based on CpG class B oligonucleotides and poly I:C alone or combined with an oil adjuvant. Vaccine **30,** 4828-4834.

Tobita K. (1975). Permanent canine kidney (MDCK) cells for isolation and plaque assay of influenza B viruses. Med Microbiol Immunol **162,** 23-27.

Torrence P.F. (1981). Preparation of a synthetic polynucleotide interferon inducer. Methods Enzymol **78,** 326-331.

Tytell A.A., Lampson G.P., Field A.K., Nemes M.M., Hilleman M.R. (1970). Influence of size of individual homopolynucleotides on the physical and biological properties of complexed rIn:rCn (poly I:C). Proc Soc Exp Biol Med **135,** 917-921.

Yoneyama M., Kikuchi M., Natsukawa T., Shinobu N., Imaizumi T., Miyagishi M., *et al.* (2004). The RNA helicase RIG-I has an essential function in double-stranded RNA-induced innate antiviral responses. Nat Immunol **5,** 730-737.

Zhang L., Liu J., Bai J., Du Y., Wang X., Liu X., *et al.* (2013). Poly(I:C) inhibits porcine reproductive and respiratory syndrome virus replication in MARC-145 cells via activation of IFIT3. Antiviral Res **99,** 197-206.

Zhao J., Xue Y., Pan Y., Yao A., Wang G., Li D., *et al.* (2019). Toll-like receptor 3 agonist poly I:C reinforces the potency of cytotoxic chemotherapy via the TLR3-UNC93B1-IFN-beta signaling axis in paclitaxel-resistant colon cancer. J Cell Physiol **234,** 7051-7061.

Figure Legends

Fig. 1: Double-stranded structure of PIC400-400CA, uPIC100-400 and uPIC50-400 molecules

Nucleotide length distributions of PIC molecules and pre-annealed components were displayed in line plots. Schematic molecule structures were attached below the plots. (A) Representative PIC400-400CA (bold line) and pre-annealed components, i.e., 0.4 kb poly(I) (gray line) and 0.4 kb poly(C) (solid line). (B) Representative uPIC100-400 (bold line) and pre-annealed components, i.e., 0.1 kb poly(I) (gray line) and 0.4 kb poly(C) (solid line). (C) Representative uPIC50-400 (bold line) and pre-annealed components, i.e., 0.05 kb poly(I) (gray line) and 0.4 kb poly(C) (solid line).

Fig. 2: Effect of PIC structure on the TLR3 signaling response

Relative intensities of human (A) and mouse (B) TLR3 responses by the corresponding HEK-Blue™ TLR3 cells plotted against the SEAP activity. Bars and error bars are the averages and SEM, respectively, of three samples. Significant responses with respect to saline are marked at the top of the bars, and the significant differences with respect to PIC400-400CA are marked with a line (**$p < 0.01$, ***$p < 0.001$).

Fig. 3: Effect of PIC structure on the RLR signaling response

Relative intensities of mouse RLR response in C57/WT MEF cells plotted against SEAP activity. Bars and error bars are the averages and SEM, respectively, of three samples. Significant responses with respect to saline are marked at the top of the bars (***$p < 0.001$).

Fig. 4: Effect of PIC structure on the IFN-β induction in human MRC-5 fibroblasts

Two groups were studied, one with cell cultures transfected with 1 μg/mL of PICs using LyoVec™ (Lipid complex), and a second group transfected with 100 μg/mL of naked PIC molecules (Naked).

Bars and error bars are the averages and SEM, respectively, of three samples. Significant responses with respect to saline in each group are marked at the top of the bars (***$p < 0.001$).

Fig. 5: Responses of the genes involved in innate immunity after delivery of PICs into human MRC-5 fibroblasts

Scatter plot of logarithmic gene expression after 24 h of transfection with PIC400-400CA against untransfected cells (A), PIC400-400CA against uPIC100-400 (B), PIC400-400CA against uPIC50-400 (C), and PIC400-400CA against ruPIC400-50 (D). R-squared is the correlation coefficient of the curve.

Fig. 6: Evaluation of PIC in mouse intranasal A(H1N1) pdm09 influenza vaccination and virus challenge

Mice were vaccinated twice by intranasal (A) (C) or subcutaneous administration (B) of the PIC, which composition is shown in the figure, and challenged with A/Narita/1/09 (H1N1) pdm09 virus. Virus titers and HA-specific IgA levels in nasal washes, and HA-specific IgG levels in serum were plotted. Bars and error bars are the averages and SD, respectively, of six samples. Significant responses with respect to the PIC-free HA vaccine are marked at the top of bars (*$p < 0.05$, ***$p < 0.001$).

Supplementary Fig. S1: Gene expression related to innate immunity after transfection of human MRC-5 fibroblasts with PIC

Representative scatter plot of the logarithmic gene expression values at 4 h after transfection of PIC400-400CA against untransfected cells (A), PIC400-400CA against uPIC50-400 (B). R-squared is the correlation coefficient of the curve.

Supplementary Fig. S2: Time course of the mouse body weight after receiving one intraperitoneal injection of 100 mg/kg PICs

Plots and error bars are the average and SD, respectively, of survived mice in each group.

Supplementary Fig. S3: Picture of agarose gel electrophoresis of PICs after incubation with or without serum

Lanes 1–8 correspond to the PICs assembled by mixing poly(I) and poly(C) molecules, as shown in the table. The positive mark of the heat & cool treatment in the table means that the PICs were heated to 60 °C for 5 minutes after mixing of poly(I) and poly(C) molecules. Serum concentrations of digested PICs are shown in the table.

Supplementary Fig. S4: Inhibition of the IFN-β production by chloroquine in human MRC-5 fibroblasts

Filter sterilized chloroquine solution was added to wells at the final concentration shown in the figure, followed by PIC transfection. The uPIC100-400 and uPIC50-400 transfected cells, together with the PIC non-transfected cells are indicated in black, gray, and white bars, respectively. Bars and error bars are the averages and SEM, respectively, of two samples.

TABLE 1: Structure and characteristics of the evaluated PIC molecules

Test material	Nucleotide length of RNA molecules						Heat treatment for NLDS adjustment‡	Tm [°C]	Storage stability in PBS at 25 °C [Month]¥	References
	Average length*			Length distribution†						
	poly(I) [kb]	poly(C) [kb]	PIC [kbp]	poly(I)	poly(C)	PIC				
long-chain PIC§	nc	nc	> 2	nc	nc	nc	nc	63	nt	(Nakano *et al.*, 2018)
PIC400-400CA	0.4	0.4	0.4	1.6	1.5	2.0	Long	63	< 1	
uPIC200-400CA	0.2	0.4	0.4	1.6	1.6	1.9	Long	63	nt	
uPIC130-400	0.13	0.4	0.4	1.4	1.5	1.8	Quick	62	nt	
uPIC100-400	0.1	0.4	0.4	1.5	1.6	1.8	Quick	62	> 4	
uPIC70-400	0.07	0.4	0.4	1.6	1.5	1.8	Quick	60	nt	
uPIC50-400	0.05	0.4	0.4	1.4	1.5	1.7	untreated	59	nt	
ruPIC400-100	0.4	0.1	0.5	1.6	1.5	1.9	Moderate	61	nt	
ruPIC400-50	0.4	0.05	0.4	1.6	1.7	1.9	Moderate	58	nt	

* The number average nucleotide length determined by size exclusion chromatography.

† Determined by the ratio of the weight average nucleotide length to the number average nucleotide length.

‡ Cooling to 30 °C at a constant rate of 2 °C / h after heating to 70 °C (Long), cooling to 30 °C for approximately 1 h after heating to 70 °C (Moderate), cooling to 30 °C for approximately half an hour after heating to 60 °C (Quick).

¥ Determined by decreasing of the NLDS of PIC.

§ Commercial product.

nt: not tested.

nc: not clear.

TABLE 2: Toxicity of single intraperitoneal administration of PIC molecules in mice

Test material	Survivals / Total		
	100 mg/kg	200 mg/kg	400 mg/kg
long-chain PIC	2/5[A] nt [B]	nt	nt
PIC400-400CA	4/5 [A] 2/5[B]	0/5[B]	nt
uPIC200-400CA	5/5[A]	2/5[B]	0/5[B]
uPIC100-400	5/5[A]	3/5[B]	0/5[B]
uPIC50-400	5/5 [A]	5/5[B]	4/5[B]

The intraperitoneal single-dose toxicity study was conducted in two parts, studies (A) and (B).
nt: not tested.

Nakano, et al., Double-stranded structure of the polyinosinic-polycytidylic acid molecule to elicit TLR3 signaling and adjuvant activity in murine intranasal A(H1N1)pdm09 influenza vaccination

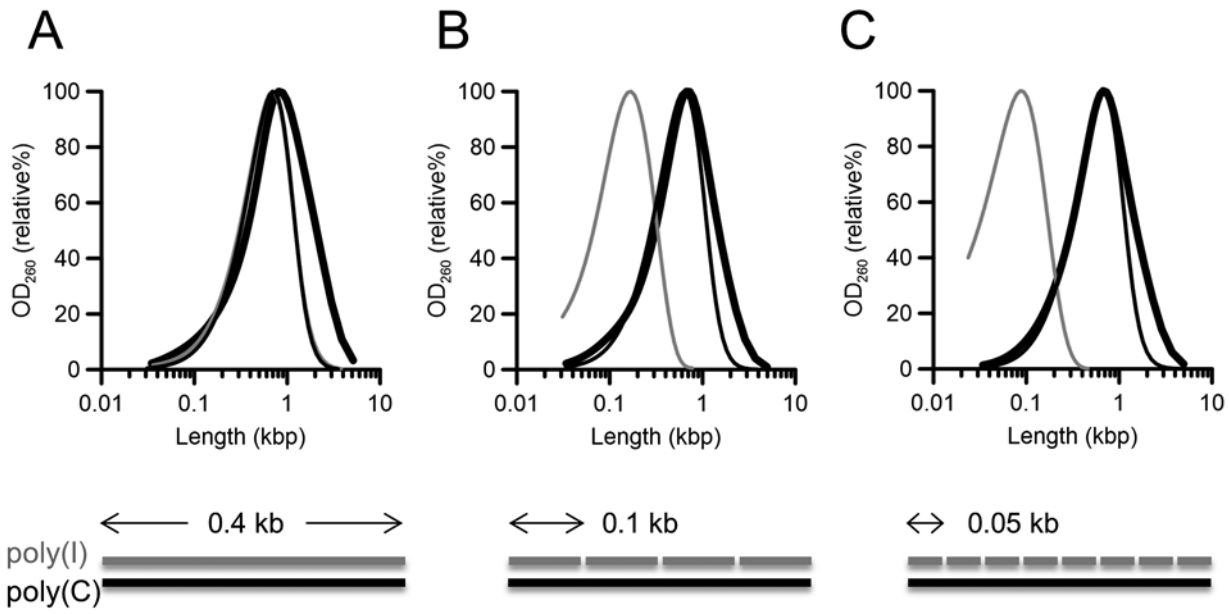

Figure 1

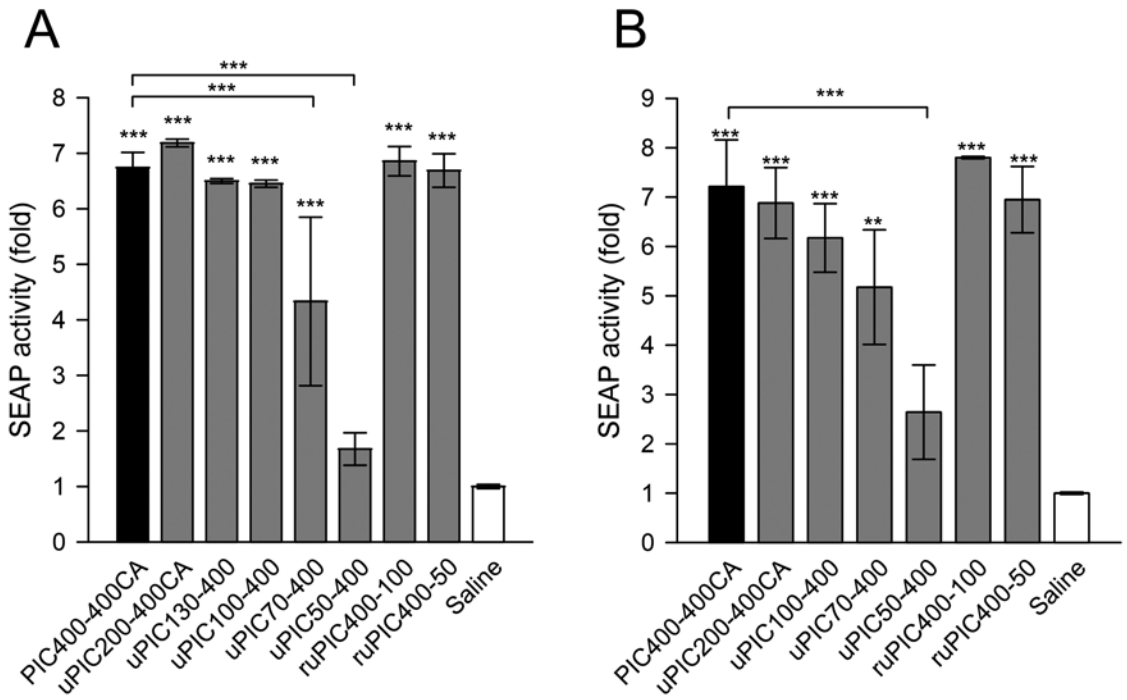
A
B
SEAP activity (fold)
PIC400-400CA
uPIC200-400CA
uPIC130-400
uPIC100-400
uPIC70-400
uPIC50-400
ruPIC400-100
ruPIC400-50
Saline
***
**

Figure 2

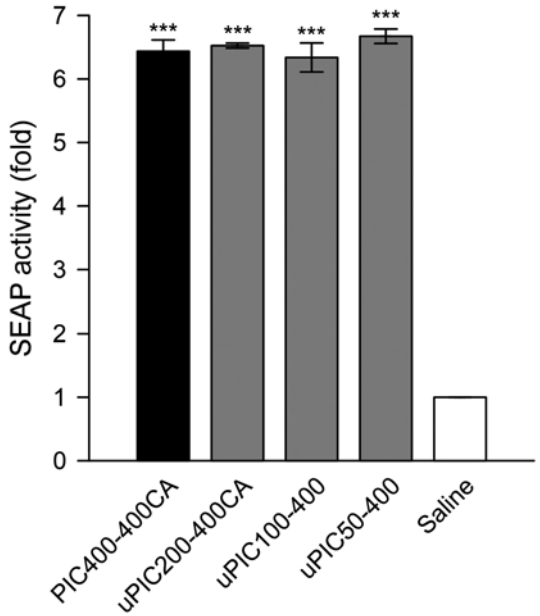
SEAP activity (fold)
0
1
2
3
4
5
6
7
***
***
***
***
PIC400-400CA
uPIC200-400CA
uPIC100-400
uPIC50-400
Saline

Figure 3

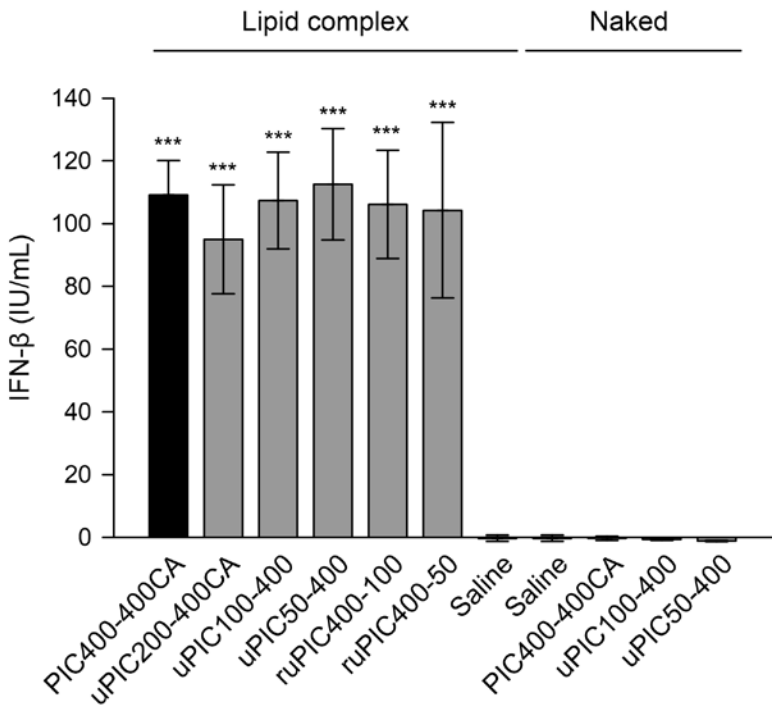
Lipid complex
Naked
IFN-β (IU/mL)
140
120
100
80
60
40
20
0
***
***
***
***
***
***
PIC400-400CA
uPIC200-400CA
uPIC100-400
uPIC50-400
ruPIC400-100
ruPIC400-50
Saline
Saline
PIC400-400CA
uPIC100-400
uPIC50-400

Figure 4

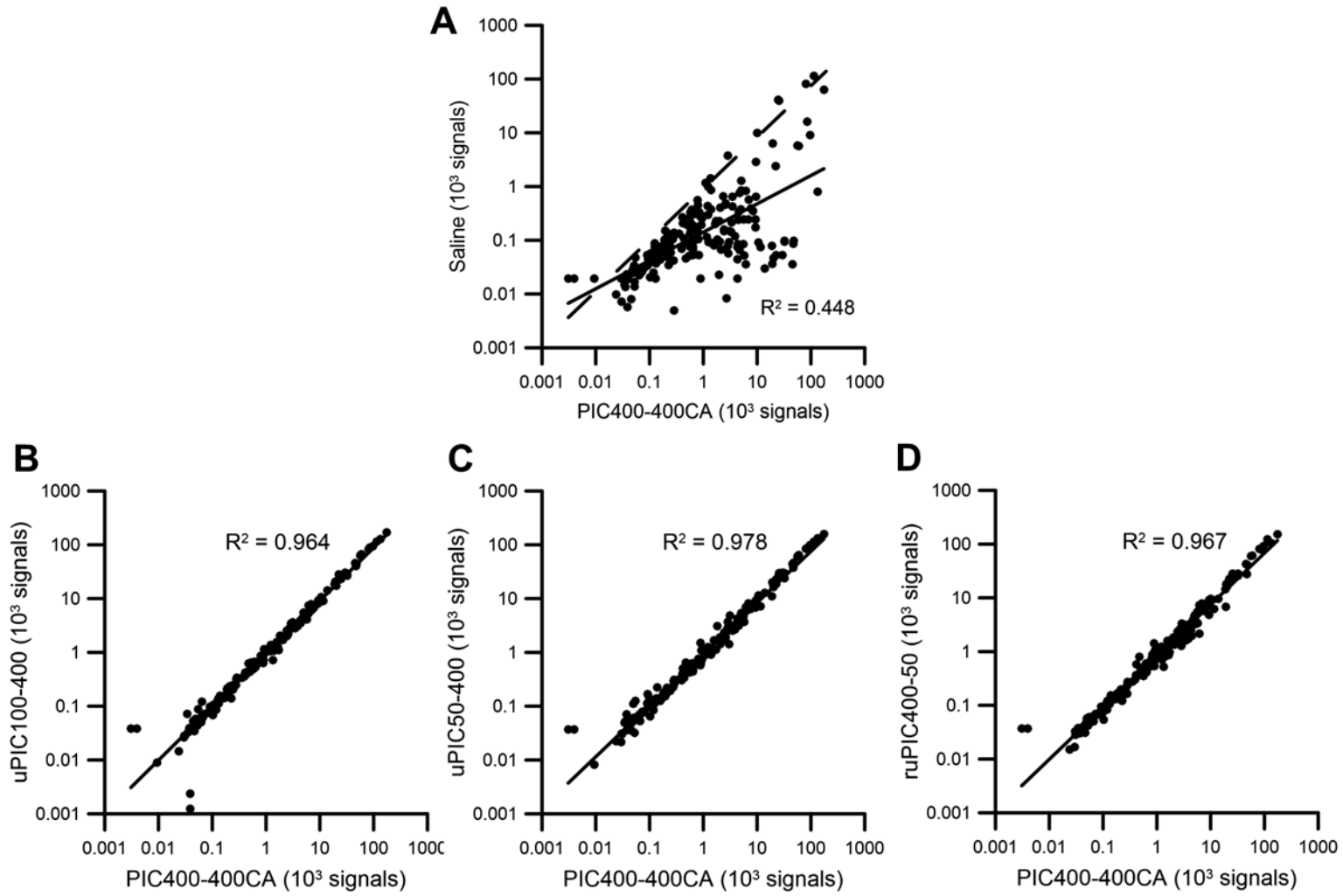
A
Saline (10³ signals)
PIC400-400CA (10³ signals)
R² = 0.448
B
uPIC100-400 (10³ signals)
PIC400-400CA (10³ signals)
R² = 0.964
C
uPIC50-400 (10³ signals)
PIC400-400CA (10³ signals)
R² = 0.978
D
ruPIC400-50 (10³ signals)
PIC400-400CA (10³ signals)
R² = 0.967
0.001
0.01
0.1
1
10
100
1000

Figure 5

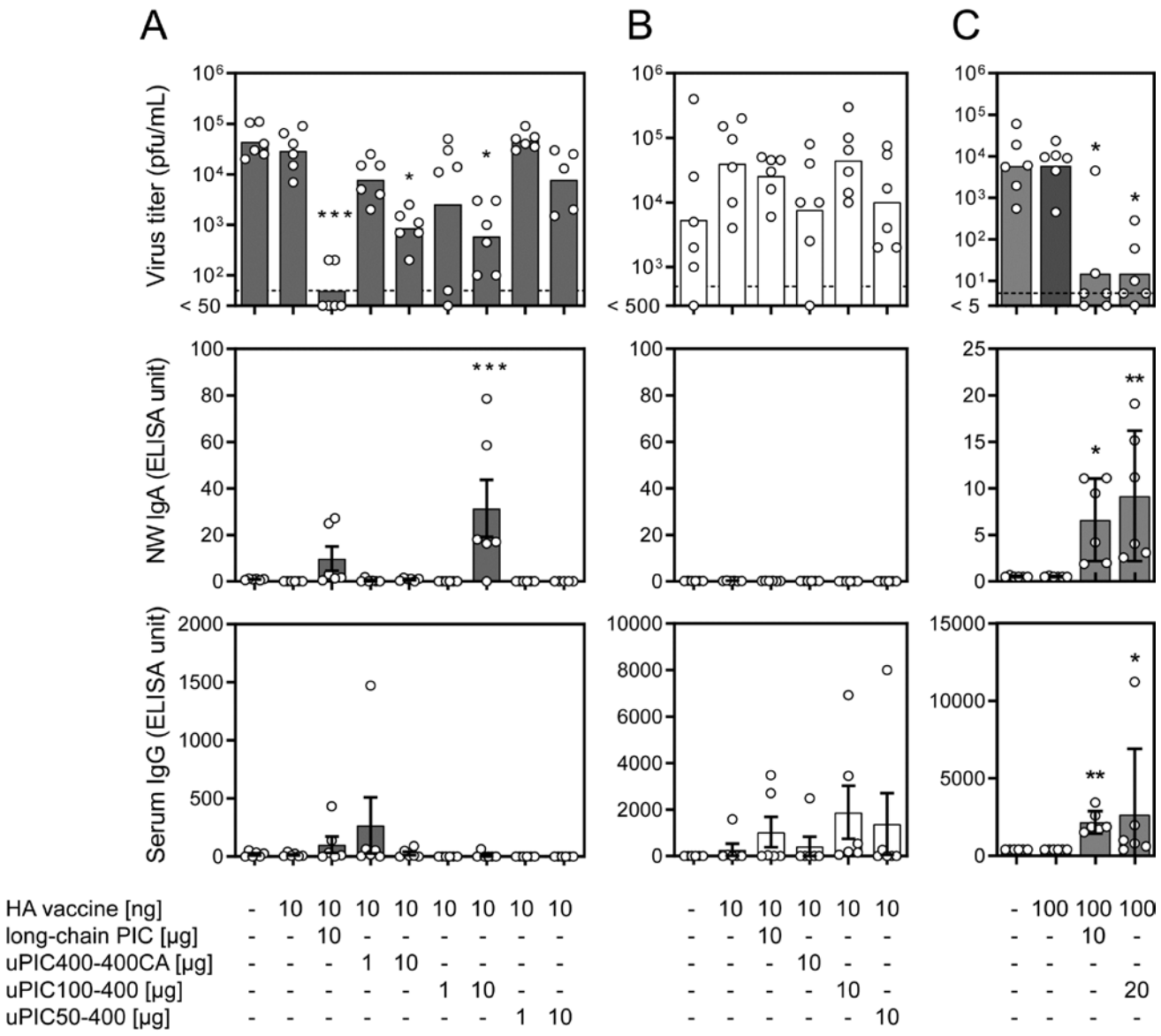
A
B
C
Virus titer (pfu/mL)
NW IgA (ELISA unit)
Serum IgG (ELISA unit)
< 50
< 500
< 5
HA vaccine [ng] - 10 10 10 10 10 10 10 10 - 10 10 10 10 10 - 100 100 100
long-chain PIC [μg] - - 10 - - - - - - - - 10 - - - - - 10 -
uPIC400-400CA [μg] - - - 1 10 - - - - - - - 10 - - - - - -
uPIC100-400 [μg] - - - - - 1 10 - - - - - - 10 - - - - 20
uPIC50-400 [μg] - - - - - - - 1 10 - - - - - 10 - - - -

Figure 6